TURBULENT FLOW CALCULATIONS FOR COMPLEX AIRCRAFT GEOMETRIES USING PRISMATIC GRID REGIONS IN THE SAUNA CFD CODE.

A J Peace, J A Chappell, J A Shaw
Aircraft Research Association Limited, Manton Lane, Bedford. MK41 7PF. UK.

Abstract

This paper is concerned with the use of prismatic grid regions to allow the modelling of viscous flow around complex aircraft configurations. In the present context, the use of such grids is within the SAUNA CFD code, which possesses an extremely general hybrid mesh framework. The addition of prismatic grid regions to the existing multi-block and unstructured grid regions gives a logical extension to the overall meshing capabilities of the code, wherein an optimum amalgamation of grid types is used within a global mesh consistent with configuration complexity. It is shown that prismatic grids provide an accurate and efficient route to flow modelling, through analysis of datum solutions on simple test cases. A view of the overall scope of hybrid grids for viscous flow is then given through the addressing of a complex aircraft geometry.

Introduction

Computational Fluid Dynamics (CFD) codes are now a key feature of virtually all aerodynamic design processes for transport and military aircraft, as well as weapon configurations. These codes provide both qualitative and quantitative information within a design exercise, thereby promoting a critical reduction in the lead time for a design. Predictions from the software allow the efficient elimination of a number of possible design options at an early stage, enabling specific and detailed tunnel testing to take place on a small number of remaining designs. Within this design process, CFD is being asked to address configurations of increasing geometric complexity. At this leading edge of the use of CFD, the input to a design is principally a qualitative one, with confidence being placed on relative predictive capability rather than absolute. To make further advances, a quantitative capability and therefore a viscous flow capability must be sought. This implies major challenges to CFD in a number of areas. Key amongst these is the need to generate computational meshes around arbitrarily complex configurations which enable the accurate and efficient computation of viscous flow.

The Aircraft Research Association (ARA) has focused on this area over the past few years. This effort has matured into a hybrid mesh generation philosophy, a strategy based on the use of grids composed of both block-structured (multi-block) and unstructured (tetrahedral) mesh regions.

The move into hybrid grids was seen at the time as a means of extending the scope of the highly successful multi-block method[1,2,3] into a more complex geometric environment. In this framework, isolated regions of unstructured mesh are embedded within a predominantly block-structured mesh to achieve the added geometric flexibility. It is strongly believed, based on good evidence[4,5], that the hybrid mesh approach gives the best route to combining geometric complexity with accuracy, efficiency and ease of use. The SAUNA (Structured And Unstructured Numerical Analysis) CFD system, which has been developed at ARA based on this hybrid mesh philosophy, has been used extensively over the past ten years, originally for Euler computations on multi-block grids, but more recently for Euler computations on hybrid grids[4] and Navier-Stokes computations on multi-block grids[6,7].

In seeking the best route to creating meshes around complex configurations suitable for viscous flow computations, the use of prismatic grid regions has been addressed, this additional grid type fitting in naturally to the hybrid mesh framework. For geometric components which are sufficiently complex that they require an unstructured surface (triangular) mesh discretisation, the 'structured extension' of this mesh away from the surface forms layers of prisms. The regular nature of such a semi-structured grid normal to the surface is seen as being preferable to a fully unstructured approach in terms of both accuracy and efficiency. Simple algebraic turbulence models are also easily applied. A number of workers, for example Kallinderis et al[8], have examined the benefits of combining prismatic grids in the near-field with unstructured grids in the far-field to achieve an attractive route to viscous flow modelling. However, it is believed that the more general hybrid mesh framework within SAUNA, with its predominant use of block-structured mesh, allows a still more attractive route. In combining multi-block, prismatic and unstructured grid regions, an overall philosophy of achieving wide geometric scope without compromising

desired accuracy and efficiency requirements is maintained for viscous flow.

It is the purpose of this paper to present some preliminary results which both demonstrate the benefit of using prismatic grid regions over a fully unstructured approach and show some early indication of the capabilities which the modified SAUNA system will have to offer in terms of viscous flow modelling. A brief description of the functionality of the software is given in the following section along with the basic methodology used, particularly in terms of the use of prismatic grids. Fine details are cited to other references. Two simple configurations are examined to demonstrate the relative accuracy and resource requirements of prismatic grids compared to multi-block and fully unstructured grids. A complex configuration is also addressed, namely a wing/body/foreplane geometry with underwing weapon, in both inviscid and viscous mode, to highlight the purpose of prismatic grids within a hybrid grid framework. Finally, a few concluding remarks are made and a brief statement of current and future work on further development of the system is given.

Overview of SAUNA system

Grid Generation

SAUNA has three grid types at its disposal - block-structured, prismatic and unstructured - which in general are combined together to form a hybrid mesh. A natural hierarchy of grid types is always applied for any given configuration:

(i) form global block-structured grid, wherever this can easily be achieved.

(ii) embed local block-structured grid, wherever possible.

(iii) generate prismatic grids away from remaining surfaces.

(iv) employ unstructured grid in remainder of domain.

The first two decisions, (i) and (ii), are the most critical, as the use of block-structured grid is always preferred based on accuracy and efficiency grounds. The decision is not purely based on what is technically possible, however, as the user-time required to create the grid is a key issue within the design environment. Therefore, block-structured grids are used in all regions of the flow domain wherever they can easily/quickly be generated. Points (iii) and (iv) then follow in a rational manner. Note that unstructured grid regions never abut component surfaces.

It should be stressed at this juncture that automation is a key feature of the software, again for consistency with design timescales. This implies that automation should be considered in the above decision making process, as well as in the individual techniques used. This aspect of the system, which is clearly one of artificial intelligence level, is still in its early stages and it is currently the situation that user experience plays a key role in decision (i) and to a lesser extent decision (ii). As will become clear, however, once these decisions have been made, a high degree of automation ensues in the rest of the system.

The structured grid component of SAUNA is based on the multi-block approach which has been well-documented over the past ten years[9], for both inviscid and viscous modelling levels. The relevant domain is automatically decomposed into a number of blocks, which are arranged to give an optimum grid topology for each geometric component. The basic mesh generation on surfaces and in the field is performed using the elliptic equations approach. High quality grids, suitable for inviscid flow, are normally generated as default, but if required these can be edited interactively. For viscous flow, selected blocks, based on user-defined surfaces, are refined in appropriate directions using a transfinite interpolation technique, this being more suitable for highly compressed grids.

If grid regions other than structured are to be used for the complete configuration, then an appropriate subset of the configuration is first meshed using the above techniques. Regions are then removed, based on geometric input, and integrity with the target geometry is achieved by adding components within this void. These added components may then have local structured or prismatic grid regions, depending on geometry complexity. In the former case, the above procedure is followed, in the latter a surface triangular discretisation is obtained using a pseudo Delaunay algorithm in tandem with an automatic point addition procedure[10]. Layers of prismatic grid are generated through a marching method, starting from the component surface and propagating outwards to an outer boundary, the exact shape or location of which cannot be predetermined[11]. Each subsequent layer is added sequentially based on the current layer. The precise direction of propagation follows a computed 'normal' vector which is calculated for each point based on a weighted average of the normals to surface triangles meeting at that point. This is then smoothed with its neighbours to eliminate sharp discontinuities, but at the expense of strict orthogonality. An average marching distance for each layer is computed, based on user input and therefore being relevant to inviscid or viscous flow. This is subsequently modified by a function based on

local surface curvature to ensure high grid quality, particularly in concave regions.

Prior to meshing remaining voids in the global flow domain, an interface or buffer region must be generated local to the outer boundary of the void. This is required for two reasons. Firstly, the triangular faces of the three-dimensional tetrahedral grid are not compatible with the quadrilateral faces of the structured grid: a layer of pyramidal elements are added to alleviate this problem. Secondly, in satisfying boundary integrity within the three-dimensional Delaunay procedure, grid edges may be interchanged and points may be added. The structured (now pyramidal) and prismatic boundaries must be protected from this process to avoid incompatibility with the local grid structure. This is achieved by adding a single layer of tetrahedra to the complete void boundary in a precise manner. A three-dimensional tetrahedral grid can then be generated using the equivalent of the unstructured surface techniques[12]. Both this technique and the buffer creation are automatic.

Flow algorithm

The flow algorithm is of the vertex-storage finite-volume type and is based on the work of Jameson et al[13] and Radespiel[14]. The spatial discretisation of the inviscid terms in the flow equations reduces to a balancing of fluxes through the faces of overlapping control volumes, which are defined as being the union of all polyhedral elements (cells) which meet at a common vertex. Thus, within a structured block the control volume is composed of eight hexahedra, with a natural extension to all other grid regions. The viscous terms are computed using a two-stage process. Firstly, the stress tensor is evaluated at cell centres using Green's theorem applied to the surface of each cell. Secondly, viscous fluxes are balanced using an auxiliary control volume formed from the centroids of the individual cells which comprise the original control volume. Therefore, inviscid and viscous contributions to the governing Navier-Stokes equations are collected at a common vertex, but using differing control volumes. The full Navier-Stokes equations are addressed rather than a thin shear layer form. A zonal approach is followed whereby viscous effects are only included in grid regions (structured or prismatic) adjacent to selected solid surfaces and in the ensuing wake regions.

An anisotropic dissipation model is used as datum, whereby scaling factors based on the wave speed for each individual grid edge, and modified by cell aspect ratio are used in the edge difference accumulation process. The treatment of artificial dissipation is critical to obtaining accurate solutions to the governing equations, so that predictions are not corrupted by large non-physical effects. To this end, research has been, and is still being undertaken to further limit the magnitude of the dissipation terms below their datum level. A number of boundary conditions are available within SAUNA, including ones relevant to powered aircraft simulation (engine compressor face and jet efflux). The discretised equations are marched in time to a steady state using a 5-stage Runge-Kutta scheme with local time stepping, residual smoothing and, for inviscid simulations, enthalpy damping. For efficiency, the viscous terms are evaluated only at the first of the five stages and then frozen for the remaining stages. In addition, a full multi-grid technique is used. Convergence can be monitored by residual level or by stabilising of forces on selected components of the configuration. Within the coding of these procedures, full advantage of the grid structure in both block-structured and prismatic grid regions is taken in terms of vector processing. Also, unstructured data connection entities are 'colour-coded', again for efficient vector speed-up.

The current level of turbulence modelling for viscous flow simulations is the Baldwin-Lomax algebraic model, with modifications to ensure continuity of turbulent viscosity coefficient at trailing edges. Transition from laminar to turbulent flow is fixed in all the calculations described in this paper, defined either from experimental testing (roughness bands) if available or by estimates from an Euler solution. A gradual phasing in of turbulence over, say, 5% local wing chord is normally applied. The implementation of the model within a structured block or a prismatic grid region is relatively straightforward, although measures to ensure a degree of smoothness in the development of the turbulence length and velocity scales are advisable for improved robustness.

Details of the above techniques can be found in References 15, 16 and 17.

Results and Discussion

To demonstrate the relative accuracy of prismatic grids as compared to other grid types and to highlight the use of prismatic grids within a general mesh framework, three configurations are addressed.

RAE 5225 aerofoil

In this example, a supercritical aerofoil section[18] is used to create a simple geometric environment. Although the basic geometry is two-dimensional, a three-dimensional geometry is created by reproducing the section in the spanwise direction to produce a plane wing without sweep or taper. A datum structured grid of C-topology was generated suitable for turbulent flow,

with chordwise plane dimensions 257 x 65 and 3 planes being stacked in the spanwise sense. A purely prismatic grid was generated by bisecting each hexahedral cell to create two prisms with triangular faces parallel to the aerofoil surface or the wake centreline. The two grids, therefore, have coincident points but differing discretisations.

Flow solutions from the Navier-Stokes method were obtained on both these grids at $M_\infty = 0.735$, $\alpha = 1.57°$ and Re = 6 million. The surface pressure distributions are shown in Figure 1, where it can be seen that only minor differences are apparent between the two solutions. Examination of the skin friction coefficients on the upper surface in Figure 2 adds further confirmation that there is no obvious loss in accuracy in a prismatic discretisation as compared to a hexahedral discretisation. The run time per point for the former is 2.04 times that for the latter, however, clearly showing the enhanced efficiency of the structured grid type. It would have been illuminating to add a fully unstructured grid into this viscous flow study. The generation of such a grid is not straightforward: in fact, the Delaunay technique used in SAUNA is not capable of creating highly compressed tetrahedral elements adjacent to solid surfaces, as would be required for a viscous flow simulation. Moreover, to the authors' knowledge no general method has been proven based on this type of technique. Of course, along with accuracy considerations, this is a reason why many unstructured mesh experts are turning to prismatic grids.

M6 wing

A genuine three-dimensional geometry is examined in the second instance - the ONERA M6 wing [19] . To enable a comparison of grid types to be made to supplement the above example, an inviscid flow (Euler) exercise is undertaken. To this end two grids were generated - a purely unstructured grid and a hybrid prismatic/tetrahedral grid. In the latter case a near-field prismatic region adjacent to the wing is combined with a far-field tetrahedral grid. The same surface triangular discretisation, generated by the method of Reference 9, is used for both the purely unstructured grid and as the initial surface for the prismatic region in the hybrid grid. In the hybrid grid, eight layers of prisms are used, with initial surface 'height' chosen to be close to that of the unstructured grid. A view of this prismatic region is shown in Figure 3. The total number of points in those two grids are 103K for the unstructured and 228K for the hybrid. The main cause of the larger number of points in the latter grid is the C-type topology that was used for the prismatic region. The presence of a wake plane in this topology implies that the density of points in both grid regions downstream of the trailing edge is much greater than in the unstructured grid case. Although grids of C-topology are not essential for inviscid flow computations, they are felt to be essential for viscous flow computations, hence their use in this comparative exercise. Therefore, two grids have been generated, each of a different type, but with closely matched point densities in the neighbourhood of the configuration surface.

The surface pressure distributions at various spanwise stations predicted from the two grids, at $M_\infty = 0.84$ and $\alpha = 3.06$, are shown in Figure 4. Although experimental data does exist for this flow condition, its inclusion on the figure is not thought to be helpful for present grid comparison purposes at an invisicd flow modelling level. It can be seen that the hybrid grid is giving consistently higher suction peaks on the upper surface, followed, on the inboard wing, by a stronger and more rearward swept shock wave and a stronger and more forward normal shock. The differing shock positions lead to a more inboard coalescence point from the hybrid grid and a stronger normal shock on the outer wing. The higher suction peaks and ensuing swept shock strengths from the hybrid grid are seen as a clear indication that a more accurate inviscid flow solution is being predicted by this grid than that from the unstructured grid. This demonstrates the accuracy advantage of a near-field prismatic grid over a tetrahedral grid.

Focusing on resource requirements the total memory per point for the unstructured grid region was three times that for the prismatic grid region. In terms of grid connectivity information, this factor was seventeen for the current example. It can be shown theoretically that this latter figure lies between four (one layer of prisms) and seventy (infinite number of layers), so the observed factor for eight layers fits in sensibly with these bounds. The equivalent ratio observed for run time per point was 1.2, although it should be stated that the 'prismatic subroutines' in the flow code have received little attention in terms of optimisation. In addition, the rate of convergence is also an important factor in overall run time and it can be shown theoretically that for the same set of points the time step for an unstructured grid is three times smaller than that for a prismatic grid, implying a three-fold reduction in the convergence rate. Therefore, there are clear efficiency benefits with the use of prismatic grids over unstructured grids, to be considered alongside the above accuracy benefits. For comparison purposes, the total memory per point for a structured grid is three quarters that for a prismatic grid, and the run time per point is less than half with an additional factor of three quarters coming from the relative convergence rates.

Wing/body/foreplane with underwing weapon

The final configuration examined is a complex geometrical case, in order to give a view of the practical use of hybrid grids in this type of environment. The baseline configuration is a wing/body/foreplane research model[20], which has been examined previously with the SAUNA code and has been reported in detail in Reference 4. The foreplane setting is such that a high quality block-structured grid can be generated for the aircraft geometry. The geometrical situation is complicated by the addition of a single, finned weapon, positioned under the main wing. It would be extremely difficult and time consuming, if not impossible, to generate a high quality block-structured grid for the aircraft/weapon combination.

Therefore, within the SAUNA hybrid mesh philosophy, a structured grid was generated around the parent aircraft alone and a region was then removed in the neighbourhood of the physical location of the weapon, to create a void. As discussed earlier, the weapon itself was now assessed as to whether it should possess either a local structured or prismatic grid. For the current weapon geometry, a high quality block-structured grid could have been generated, but for the purposes of this demonstration a prismatic grid was used. The weapon and accompanying local grid were then inserted into the void of the parent grid. A buffer region and unstructured grid region were then added to complete the global hybrid grid. The final surface grid is shown in Figure 5.

This case amply demonstrates the building block route to configurations of arbitrary complexity that are possible within the SAUNA system, through the use of optimum grid types to maximise grid quality and efficiency. Although the weapon does not intersect the parent aircraft in this case this is not a limitation of the method. Any number of intersecting bodies, each with their own local grid, can be appended to the baseline geometry.

As the focus of this paper is on viscous flow using prismatic grids, two grids have been generated. The first is suitable for inviscid flow and the second allows the modelling of viscous effects around the weapon, that is, within the prismatic grid region. The local grid topology in the prismatic region is of O-type and recalling the discussion from the previous example, this is not ideal for a viscous flow computation, due to its poor wake modelling characteristics. In terms of providing a demonstration of capability, this is not thought to be critical for present purposes. However, a more rigorous validation exercise would require a prismatic region of C-structure, this being within the functionality of the system, but not readily available for the current exercise. The inviscid flow grid was composed of 861K points with 744K being in the structured blocks, 65K in the prismatic region in eight layers and 52K in the unstructured/buffer region. A view of this grid highlighting the weapon and its local prismatic grid is given in Figure 6. The viscous flow grid was composed of 25 layers of prisms, suitably compressed towards the weapon surface, giving a total grid of 991K points.

Flow solutions were obtained at $M_\infty = 0.9$, $\alpha = 6°$ and Re = 6 million. Pressure shaded contours from the inviscid prediction on the wing lower surface and the weapon are shown in Figure 7. The high speed regions on the weapon (dark shading), both terminated by a shock wave, and the imprint of the weapon interference on the lower wing surface can clearly be seen. A quantitative measure of this interference is given in Figure 8, where the wing surface pressure distribution from this solution is compared with that from a calculation with no weapon present. This latter calculation was performed on the above baseline aircraft grid with no region removed, so that the majority of the two grids are identical, thus allowing a very fair comparison.

To show a measure of the viscous effects predicted from the turbulent flow calculation, the surface pressure distribution on the weapon upper surface is plotted in Figure 9 and compared to the inviscid flow prediction. In the absence of experimental data on the weapon, a quantitative comparison is not possible, but the expected effects of shock weakening and reduced afterbody recompression in the viscous flow case can clearly be seen in the figure. Obviously a more thorough validation of this type of calculation is required and this will be performed in the near future.

Concluding remarks

The benefits of using prismatic grid regions within a general hybrid mesh philosophy have been demonstrated. Due to their semi-structured nature, these mesh regions allow high accuracy to be achieved for viscous and inviscid flow around aircraft components which are geometrically complex. They also offer significant efficiency gains over a fully unstructured grid approach. It is considered that the full potential of prismatic grids are brought to the fore when they are used alongside structured and unstructured grids, as in the SAUNA CFD code, with structured grids still being the first choice meshing route . An example of such a use has been given in this paper, but further development is required before the complete scope of general hybrid grids for complex aircraft geometries is available.

This development is in progress, accompanied by advances on the physical modelling side through the use of differential turbulence models. It is believed that the scope of simple algebraic models is fairly narrow in a hybrid grid context, in terms of both implementation and accuracy. The structural properties they require of the grid limits them to particular regions and their ability to predict even qualitative effects adjacent to complex geometrical surfaces is severely limited. Differential turbulence models provide a route to overcoming these problems. It is critical that advances in gridding and flow modelling are addressed together with efficiency issues, as added complexity in both areas implies increased computational effort. To this end, a strategy based on parallel processing using a distributed memory approach is being aggressively followed. The SAUNA flow solver already exists in a parallel version and other parts of the system are to be parallelised in the near future. All these advances will lead to a wider and more effective use of CFD in the design process.

ACKNOWLEDGEMENT

This work has been undertaken with the support of the Procurement Executive, United Kingdom Ministry of Defence. The authors would like to thank their many colleagues for offering advice and helping in the production of this paper.

REFERENCES

1. McParlin, S C, Doherty, J J and Wood, S E, ´Validation of a multi-block Euler method for supersonic flows about complex configurations`. Proc. 1993 European Forum on Recent Development and Applications in Aeronautical CFD, Paper 30, 1993.

2. Fulker, J L, Ashill, P R and Shires A, ´A theoretical and experimental investigation of the low over a supersonic leading edge wing/body configuration`, Paper 31, loc.cit. [1].

3. Doherty, J J and Parker, N T, ´Application of an Euler multi-block optimisation design method to a supersonic transport`. Proc. 7th European Aerospace Conference, 1994.

4. Shaw, J A, Peace, A J, Georgala, J M and Childs, P N, ´Validation and evaluation of the advanced aeronautical CFD system SAUNA - a method developer's view`, Paper 3, loc.cit. [1].

5. Shaw, J A, Peace A J, May, N E and Pocock, M F, ´Verification of the CFD simulation system SAUNA for complex aircraft configurations`, AIAA-94-0393, 1994.

6. Peace, A J, May, N E, Pocock, M F and Shaw, J A, 'Inviscid and viscous flow modelling of complex aircraft configurations using the CFD simulation system SAUNA', ICAS Paper 94-2.6.3, 1994.

7. Macdonald-Smith, D, ´Evaluation of the SAUNA Navier-Stokes flow solver for the W4 and B60 wing/body configurations`. ARA CR M274/1, 1996.

8. Kallinderis, Y, Khawaja, A and McMorris, M, ´Hybrid prismatic tetrahedral grid generation for complex geometrys`. AIAA-95-0211, 1995.

9. Shaw, J A, Georgala, J M and Weatherill, N P, ´The construction of component adaptive grids for aerodynamic geometries`, Proc. 2nd Int. Conf. on Numerical Grid Generation in CFD'88, eds Sengupta et al, Pineridge Press, pp 383-394, 1988.

10. Childs, P N and Weatherill, N P 'Generation of unstructured grids within a hybrid multi-block environment', in Numerical grid generation in CFD and related fields, eds Archilla et al, North Holland, pp 899-991, 1991.

11. Chappell, J A, Shaw, J A and Leatham, M, ´The generation of hybrid grids incorporating prismatic regions for viscous flow calculations`, Proc. 5th Int. Conf. on Numerical Grid Generation in CFD and related fields, eds Soni et al, Mississippi State University, 1996.

12. Childs, P N, Shaw, J A, Peace, A J and Georgala, J M, ´SAUNA: A system for grid generation and flow simulation using hybrid structured/unstructured grids`, in CFD'92, eds Hirsch et al, Elsevier, pp 875-882, 1992.

13. Jameson, A, Baker, T J and Weatherill, N P, ´Calculation of inviscid transonic flow over a complete aircraft`, AIAA-86-0103,1986.

14. Radespiel, R, ´A cell-vertex multi-grid method for the Navier-Stokes equations`, NASA TM 101557, 1989.

15. Peace, A J and Shaw, J A, ´The modelling of aerodynamic flows by solution of the Euler equations on mixed polyhedral grids`, Int. J. Num. Methods in Eng., Vol 35, pp 2003-2029, 1992.

16. Peace, A J, 'Multi-grid convergence acceleration of a cell-vertex Euler algorithm using block-structured meshes', ARA Memo 382, 1993.

17. Peace, A J and May, N E, 'A multi-grid Navier-Stokes method for block-structured grids', ARA CR M237/8/4, 1996.

18. Ashill, P R, 'Investigation of the flow over a series of 14%-thick supercritical aerofoils', Case A3 in A Selection of Experimental Test Cases for the validation of CFD codes, AGARD-AR-303, 1994.

19. Schmitt, V and Charpin, F, 'Pressure distribution on the ONERA-M6-wing at transonic Mach numbers', in Experimental data base for computer program assessment, AGARD-AR-138, 1979.

20. Stanniland, D R, 'Investigation of the flow development on a highly swept canard/wing research model with segmented leading and trailing-edge flaps', Case D5, loc.cit. [15].

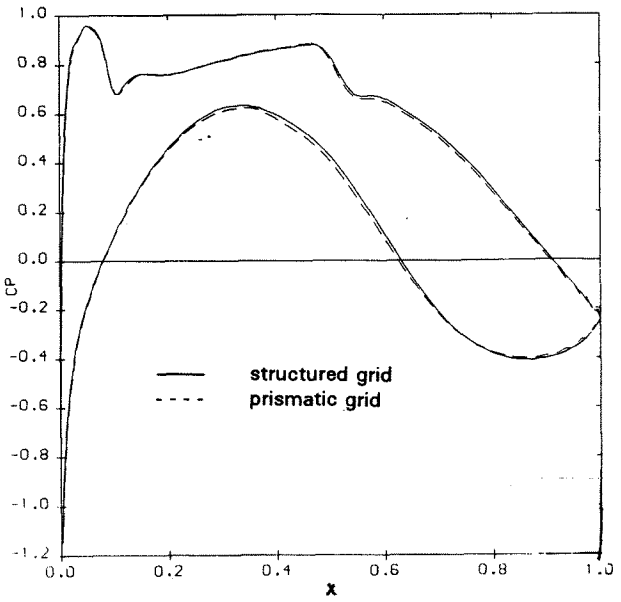

FIG 1 RAE5225 AEROFOIL, VISCOUS FLOW PRESSURE DISTRIBUTION - COMPARISON OF GRID TYPES.

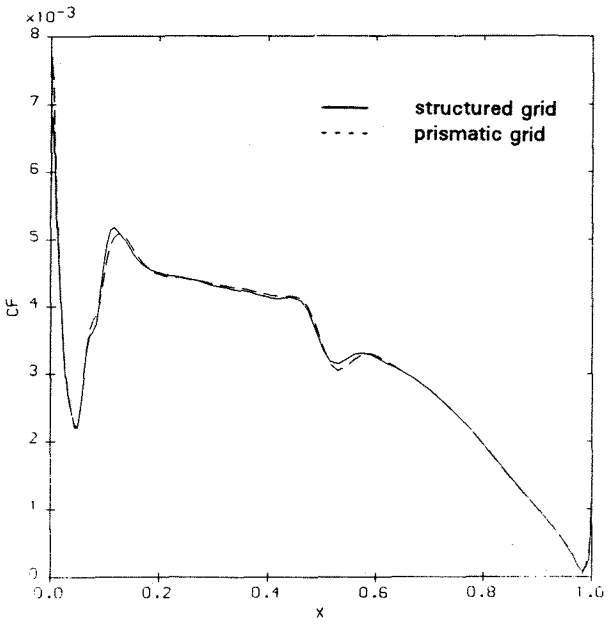

FIG 2 RAE5225 AEROFOIL, SKIN FRICTION DISTRIBUTION - COMPARISON OF GRID TYPES.

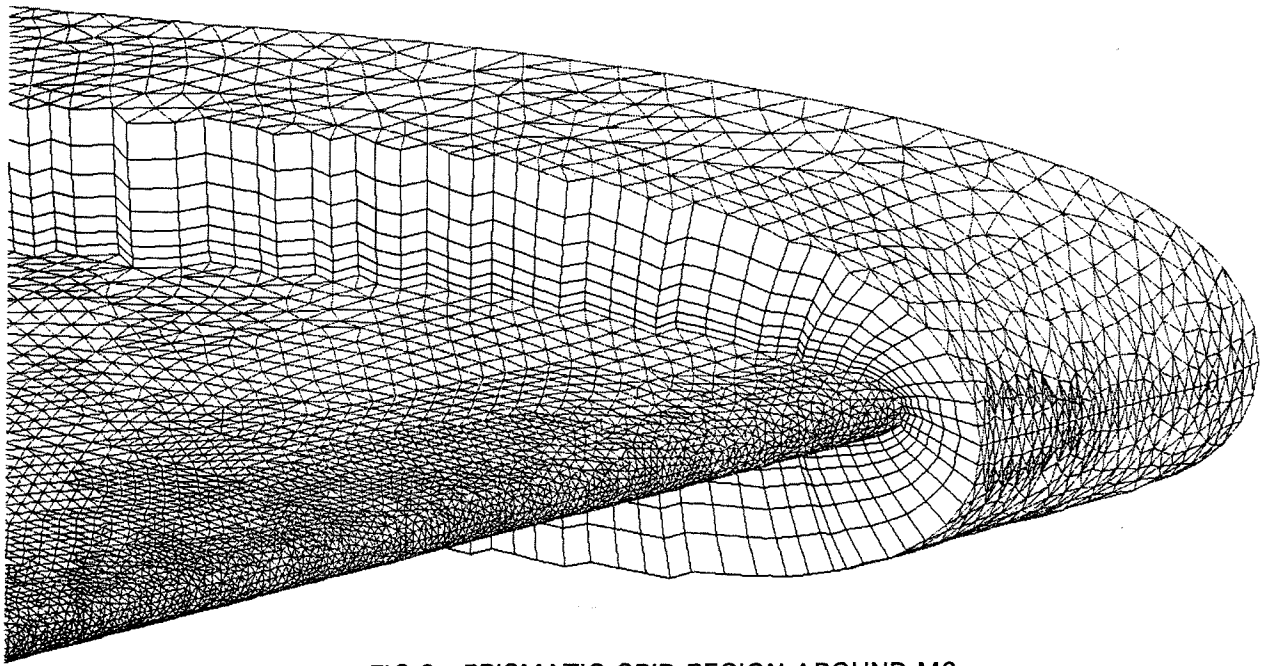

FIG 3 PRISMATIC GRID REGION AROUND M6 WING.

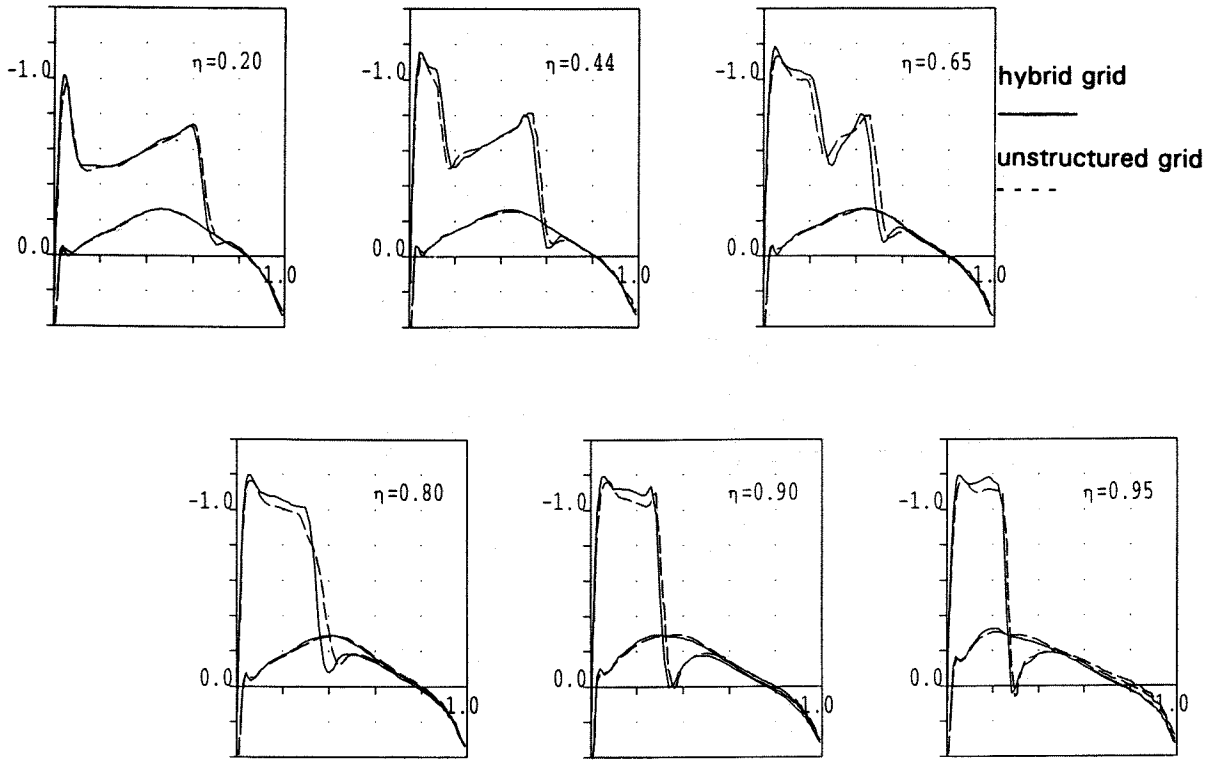

FIG 4 M6 WING INVISCID FLOW PRESSURE DISTRIBUTION - COMPARISON OF GRID TYPES.

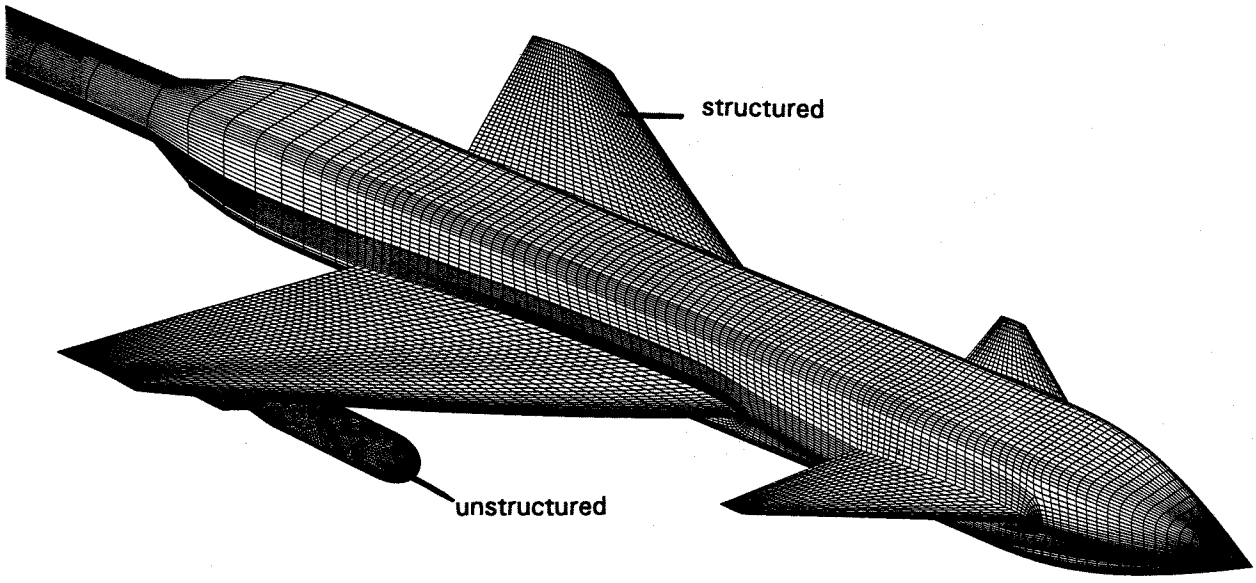

FIG 5 SURFACE GRID ON COMPLEX CONFIGURATION.

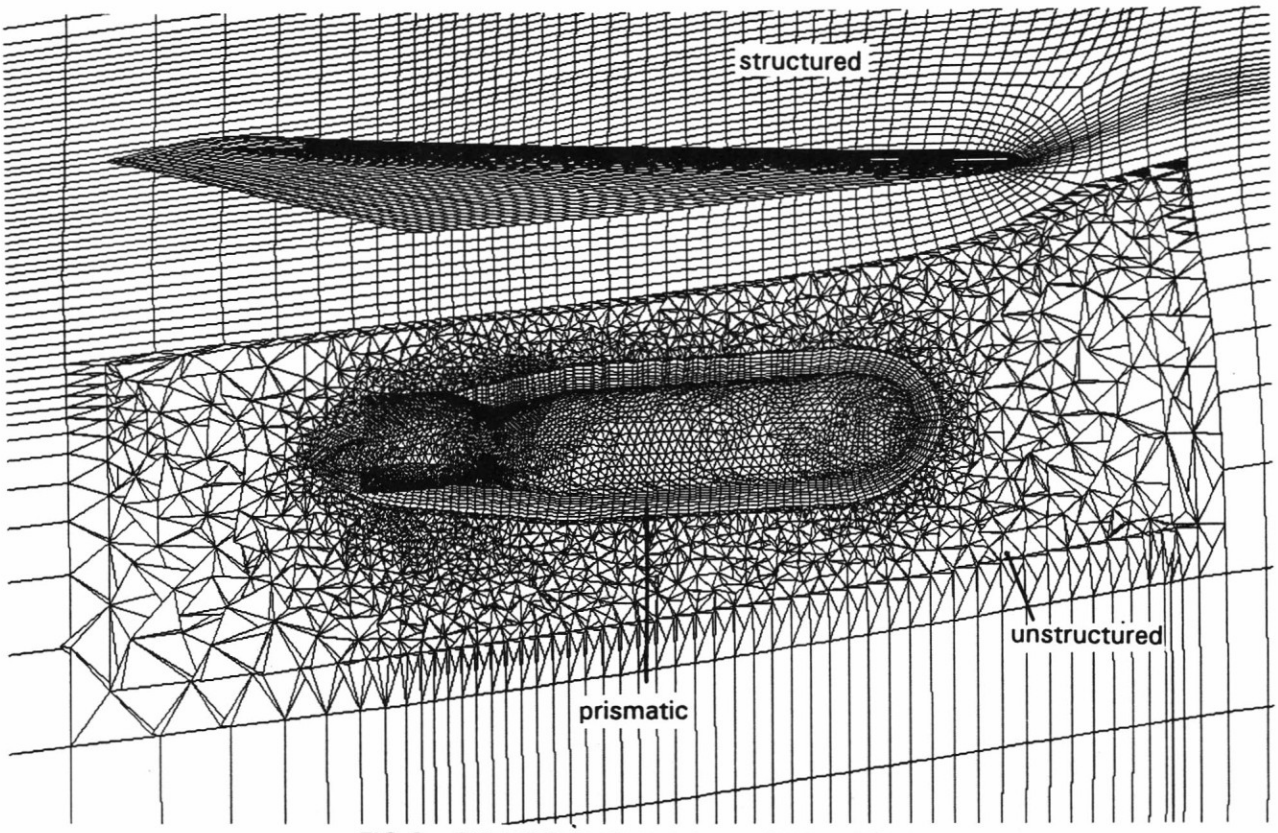

FIG 6 CUT THROUGH HYBRID GRID AROUND COMPLEX CONFIGURATION.

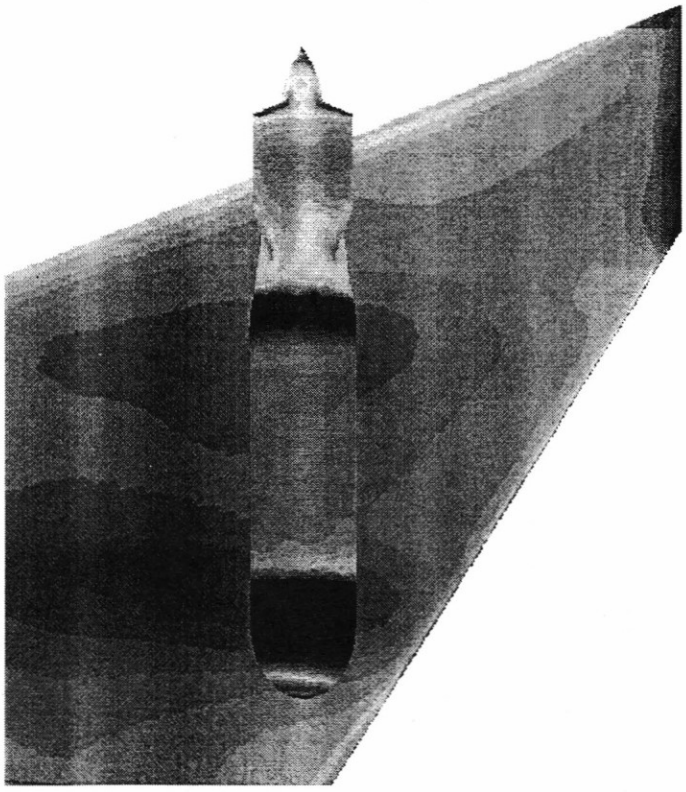

FIG 7 SHADED PRESSURES ON WING LOWER SURFACE AND WEAPON.

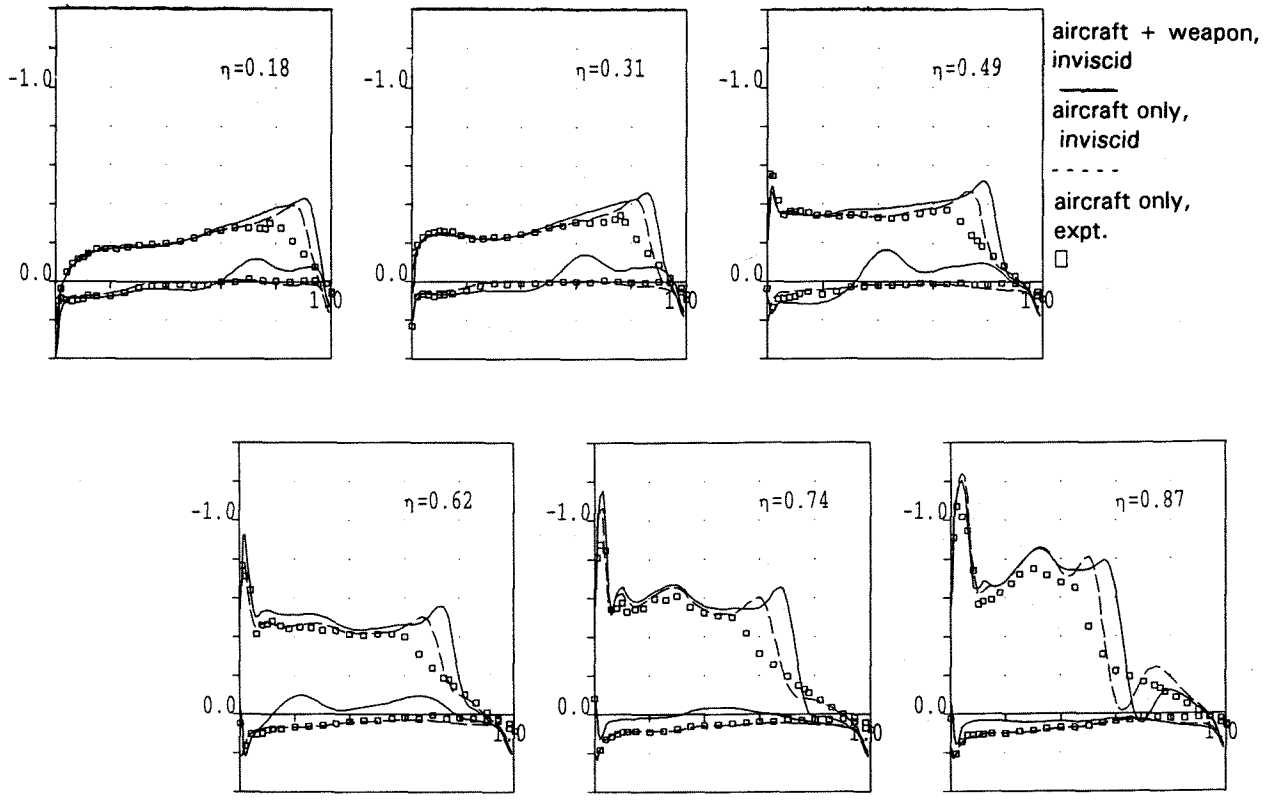

FIG 8 COMPLEX CONFIGURATION WING PRESSURES.

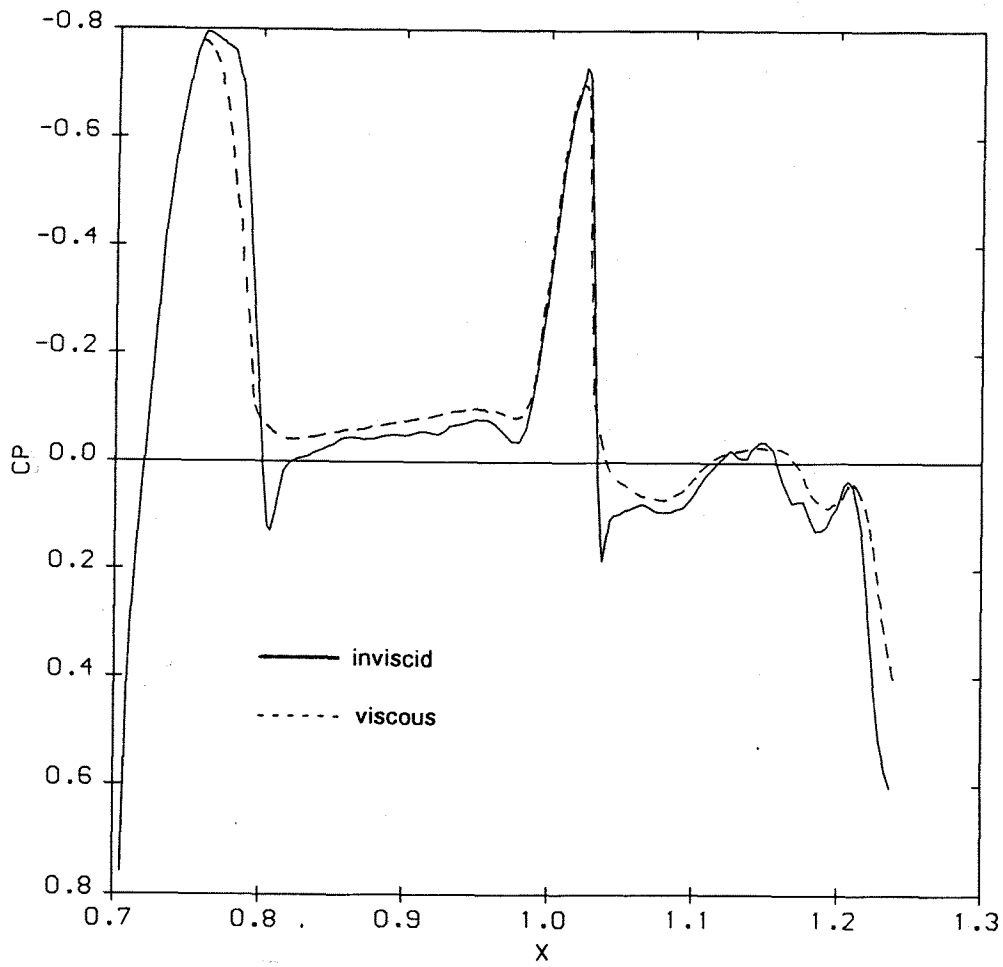

FIG 9 COMPLEX CONFIGURATION WEAPON PRESSURES (UPPER SURFACE)